e-ISSN 2320 –7876 www.ijfans.org
Vol.11, Iss.9, Dec 2022

Research Paper

Sol-gel synthesis, structural and magnetic characterization studies of spinel $CdFe_2O_4$ nanoparticles

N. Deebakaran[1,*], G. Padma Priya[1]

[1] Department of Chemistry, Faculty of Arts and Science,
Bharath Institute of Higher Education and Research (BIHER),
Chennai – 600073, Tamil Nadu, India

***Corresponding Author Email:** nadeeban4971@gmail.com (N. Deebakaran)

Address for Correspondence

N. Deebakaran[1,*], G. Padma Priya[1]

[1] Department of Chemistry, Faculty of Arts and Science,
Bharath Institute of Higher Education and Research (BIHER),
Chennai – 600073, Tamil Nadu, India

***Corresponding Author Email:** nadeeban4971@gmail.com (N. Deebakaran)

ABSTRACT

Spinel $CdFe_2O_4$ nanoparticles were synthesized using metallic nitrates and PEG using sol-gel method followed by calcination for 2 h at 600 °C. PEG performed as a surfactant. FT-IR spectral analysis, powder XRD, HR-SEM, thermogravimetry /differential scanning calorimetry (TG/DSC) analysis and vibrating sample magnetometer (VSM) were used to study the morphology, structural, thermal and magnetic properties of spinel $CdFe_2O_4$ powder. FT-IR spectral results shows that type of bonds between metals and oxygen, XRD results indicated that the resultant particles had crystalline, pure single phase monoclinic $CdFe_2O_4$ structure and HR-SEM shows that the particles are well defined spherical shaped nano particle.

Keywords: Sol-gel method; Spinel; $CdFe_2O_4$; Morphological analysis; X-ray diffraction.

e-ISSN 2320 –7876 www.ijfans.org
Vol.11, Iss.9, Dec 2022

Research Paper

1. Introduction

Nowadays, the design and synthesis of semiconductor nano-magnetic particles has the focus of the intense fundamental and applied research with special emphasis on their enhanced properties that are different from those of their bulk counterparts [1-6]. Nano-cadmium ferrite ($CdFe_2O_4$) is a normal spinel ferrite that can be applied in various fields [7-10]. Nano-$CdFe_2O_4$ exhibits ferromagnetism, and ~54% of Fe^{3+} ions occupy the A site in contrast to 0% for the bulk materials with normal spinel structures [11-13]. The enhanced occupancy of Fe^{3+} ions in $CdFe_2O_4$ is explained by a higher octahedral preferential energy of Cd^{2+} [14]. It is found that nano-$CdFe_2O_4$ can be obtained at low temperature by applying solution methods [15-20].

This process is chosen because it gives enhanced homogeneity, better control for size, shape, and degree of agglomeration of the resulting nanocrystals, simple compositional control, and low processing temperature [21, 22]. In order to obtain sols and gels with desirable properties, the control of precursor reactivity may be achieved through the addition of chelating agents such as β-diketones, carboxylic acids, or other complex ligands [23]. These characteristics, along with the chemical composition, are found to influence significantly the magnetic properties of nanoferrites [24].

The aim of this paper is to explain theoretically the reason of nano-$CdFe_2O_4$ formation when using the sol-gel process that gives a single phase at both lower sintering temperature and time than that used previously [25]. In this work, we attempt to synthesize $CdFe_2O_4$ particles by a simple sol–gel method using Polyethylene Glycol (PEG) as surfactant. PEG is a polyether compound contains hydroxyl group, which plays an important role in the dispersion process of $CdFe_2O_4$ particles. This hydroxyl group forms an ester linkage with Citric Acid which forms big polymeric structure which traps the metal salts & water and thus prevents the agglomeration of particles. The prepared nanomagnetic materials are characterized using XRD, FTIR, SEM and VSM techniques. Based on the achieved experimental results, a new model is proposed to explain the link between the use of the sol-gel process and the formation of nano-$CdFe_2O_4$ as a pure phase at low temperature. Biological studies, antibacterial and antifungal activities, also performed.

e-ISSN 2320 –7876 www.ijfans.org
Vol.11, Iss.9, Dec 2022

Research Paper

2. Experimental techniques

2.1 Materials and Methods

Fine particles of Cadmium Ferrite $CdFe_2O_4$ were synthesized by sol gel process. The chemicals Ferric Nitrate (Fe $(NO_3)_3.9\ H_2O$), Cadmium Nitrate Citric Acid (CA) and Polyethylene Glycol (PEG) (MW=40000 44000 to 54000) were used. (Source of purchase of chemicals to be mentioned) All chemicals were of analytical grade and used without purification. PEG is dissolved in deionized water. Ferric nitrate and Cadmium nitrate in stoichiometric ratio of 2:3 (quantity to be given in molarity), and CA were dissolved in deionized water separately. These solutions were added to PEG solution at 50 °C to form the sol. This sol is then heated slowly to 90 °C under constant stirring, to obtain a wet gel. The gel was kept in hot air oven for 2 days to evaporate water. Yellow solid mass was obtained. Then the product was calcined at 650 °C for 2 h. It was ground in a mortar to form a fine powder. The nature of bonds between atoms in the molecule was identified by IR spectral analysis. The phase structure analysis of products was identified using an X-ray diffract meter (PANalytical X'pert pro) of wave length (λ=0.15406 nm) in a wide range of 2θ ($10°<2\theta<70°$). The morphology of the powder was analysed by HR-SEM (FEI Quanta 200FEG). The magnetic saturation magnetization and coercivity of the powder were measured by a Vibrating Sample Magnetometer (VSM) - Lakeshore 7304 with a maximum field of 20,000 Gauss at room temperature.

2.2 Characterization

The characterization of the prepared $CdFe_2O_4$ nanoparticles was conducted by using various techniques to verify the particle size, distribution and to explore other parameters of interest. IR spectral analysis was performed using BRUKER FT IR spectroscopy. Thermal studies (TG/DSC analysis) was carried out on samples A, B, C, and D from room temperature to 1200 °C on NETZSCH STA 409 C/CD in static air atmosphere at a heating rate of 10 °C per minute. The structure of the $CdFe_2O_4$ nanoparticles was characterized by the XRD technique using X-ray diffract meter (PANalytical X'pert pro) of wave length (λ=0.15406 nm) in a wide range of 2θ ($10°<2\theta<80°$). The morphology of the powder was analysed by HR-SEM (FEI Quanta 200FEG). The magnetic saturation magnetization and coercivity of the cobalt ferrite

powder were measured by a Vibrating Sample Magnetometer (VSM) - Lakeshore 7304 with a maximum field of 20,000 Gauss at room temperature.

3. Results and Discussion

3.1 FT-IR Spectral Analysis

Fig. 1 shows the FT-IR spectra of (a) gel precursor and (b) $CdFe_2O_4$ powder precursor. The IR spectra of gel precursor sample contain a broad band between 3200 and 3400 cm^{-1} due to the O-H stretching mode of non-dissociated hydroxyl groups bonded with PEG and the intermolecular hydrogen bond [26]. Furthermore bands related to C=O and C–O stretching modes from the ester groups formed as a result of the esterification reactions that appear at ~1708 and ~1042 cm^{-1}, respectively [27]. The absorption band at 1193 cm^{-1} attributed to C-C absorption. The spectra of powder precursor shows two major sharp bands at 805 and 778 cm^{-1} that are characteristic of spinel ferrite ($CdFe_2O_4$) are observed. The higher frequency band is caused by stretching vibration of the tetrahedral metal-oxygen band (Fe–O), and the lower frequency absorption band is caused by a metal-oxygen stretching vibration in octahedral sites (Cd–O) [28]. The sharpness of these bands is correlated to the high degree of crystallinity of the obtained phase.

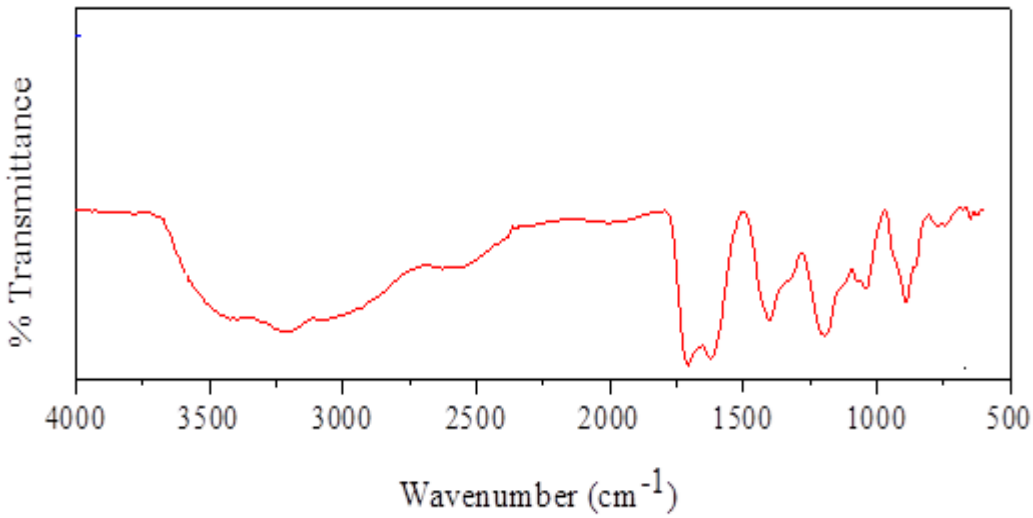

Fig. 1. FT-IR Spectra of $CdFe_2O_4$ NPs

e-ISSN 2320 –7876 www.ijfans.org
Vol.11, Iss.9, Dec 2022

Research Paper

3.2 Thermal decomposition of gel precursor

Fig. 2 shows the TG /DSC curve for the gel precursor. The first endothermic curve in DSC curve with the peak at 141 2°C, accompanied by a mass loss of about 12.8% in the TG curve is due to inner water contained in gel sample. On further heating, second at 221.9°C, third at 339.1°C and fourth at 386.6°C, endothermic curves due to liberation of nitrates, degredation of citrate ester, polymer and other organic compounds, with a mass loss of 29.6%, 20.55% and 10.77% respectively. The final endothermic curve, with a peak at 642.5 °C is due to the formation of main phase. Organic compounds are completely removed above 642.5°C and the XRD results support TG/DSC analysis with the absence of any peak related to polymer and other organic compounds.

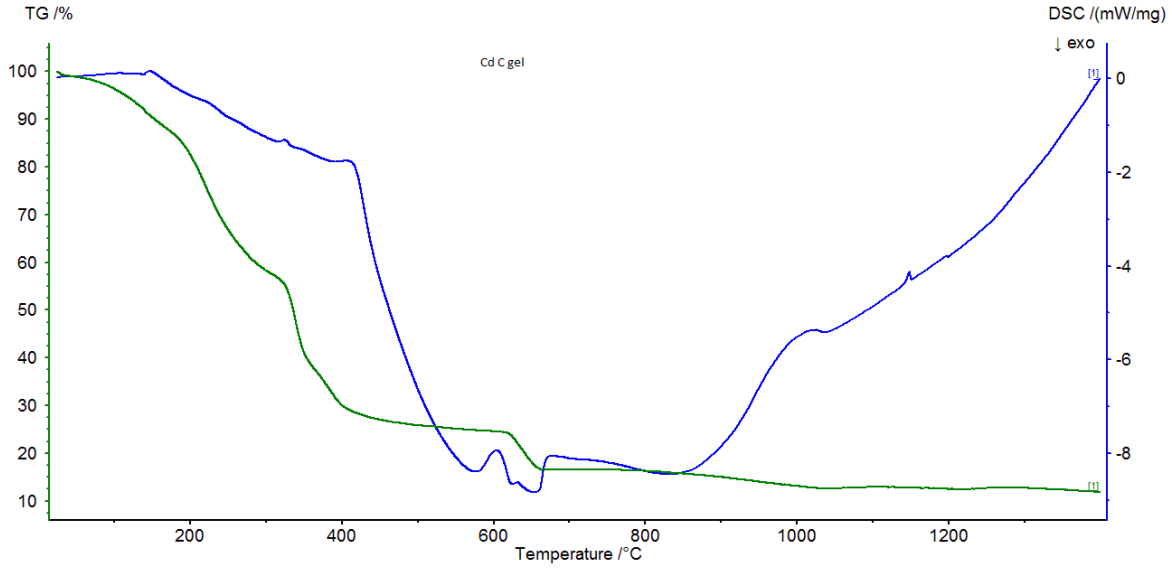

Fig. 2. TG/DSC curves of the gel precursor heated from room temperature to 1,200 °C at a rate of 10 °C per minute in air

3.3 X-ray diffraction studies

The XRD patterns of $CdFe_2O_4$ NPs is shown in Fig. 3. The pattern of the sample show prominent peaks observed at 2θ values of 30.02°, 35.13°, 43.25°, 53.16°, 57.05° and at 63.02° are indexed to (220) (311) (400) (422) (511) (440) planes respectively. These peaks belong to the

e-ISSN 2320 –7876 www.ijfans.org
Vol.11, Iss.9, Dec 2022

Research Paper

cubic spinel type lattice of $CoFe_2O_4$, which matches well with the standard XRD pattern (JCPDS Card No: 22-1086). In order to further analyze the structural change, the measured XRD patterns of the NPs were simulated based on Rietveld refinement method for all compositions Fig. 3b.

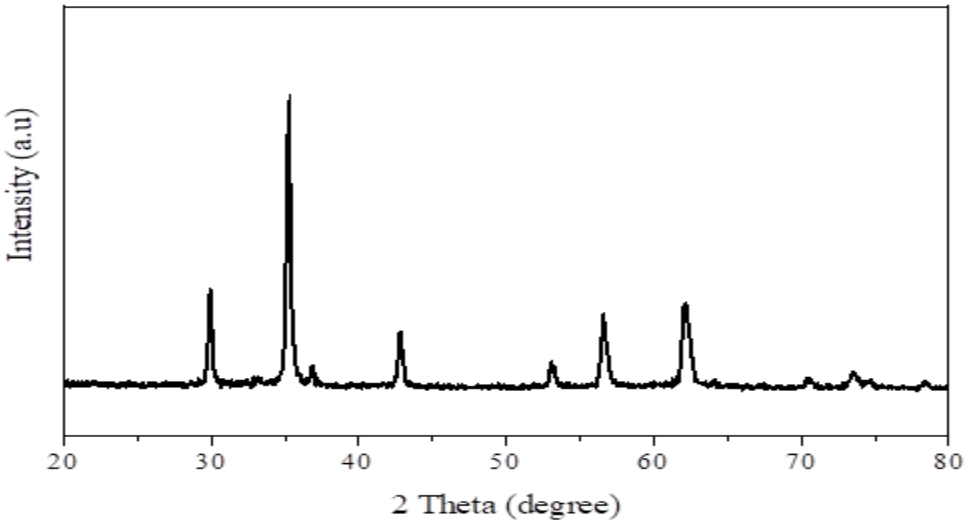

Fig. 3a. Powder XRD patterns of $CdFe_2O_4$

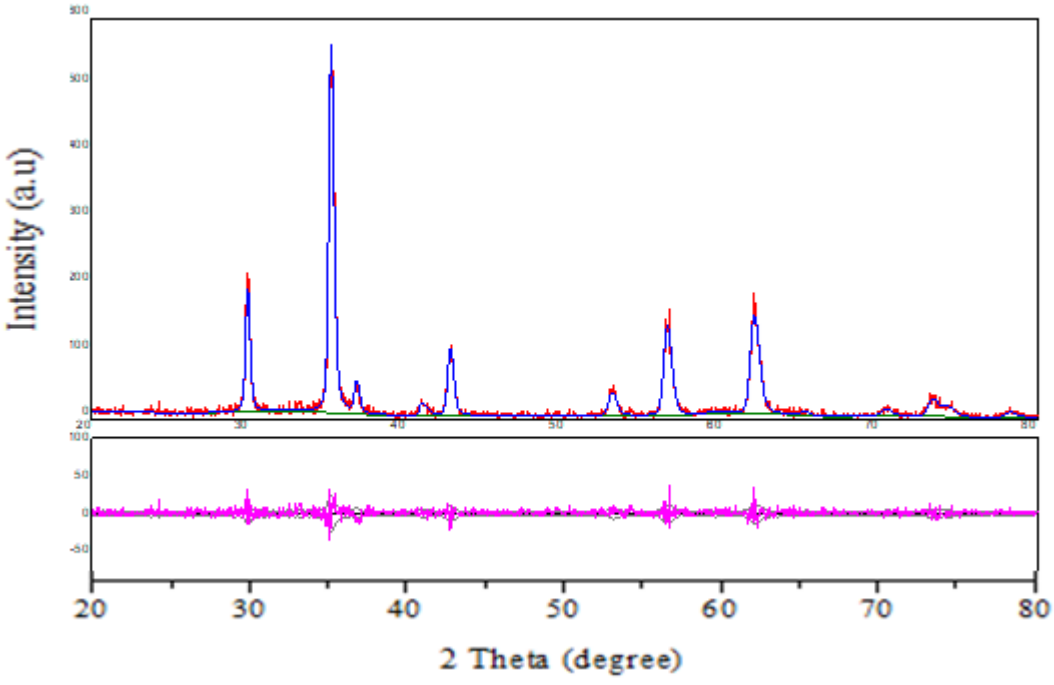

Fig. 3b. Rietveld XRD data of of $CdFe_2O_4$

e-ISSN 2320 –7876 www.ijfans.org
Vol.11, Iss.9, Dec 2022

Research Paper

3.4 HR-SEM studies

Typical HR-SEM images of $CdFe_2O_4$ powder is shown in Fig. 4. From the images, we can see the spherical shaped nanoparticles morphology with smaller sizes in the range of 20-30 nm is visible. Moreover, a smaller agglomeration occurred due to the magnetic interaction between the particles which results the aggregation followed by the agglomeration of the samples.

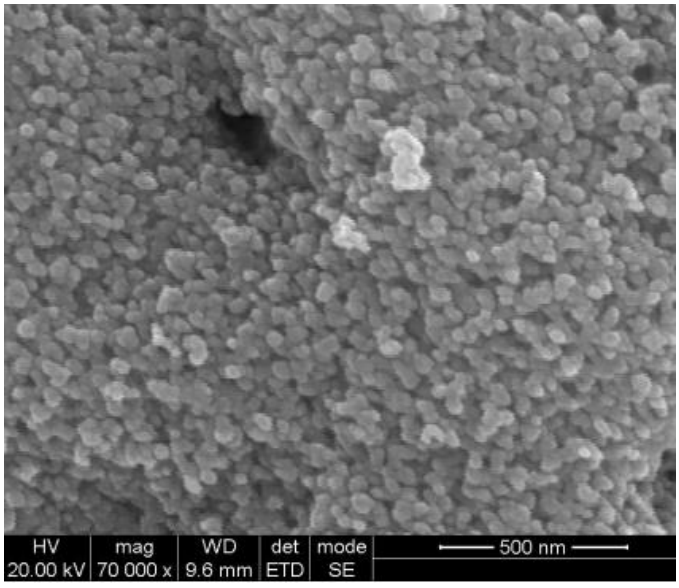

Fig. 4. HR-SEM images of $CdFe_2O_4$ powder.

3.5 HR-TEM studies

Transmission electron microscopy (HR-TEM) analysis was carried out and is shown in Fig. 5, shows the HR-TEM images of $CdFe_2O_4$ powder with diameter ranging from 16-20 nm. It is obvious that the sphere-like nanoparticles are uniform in size, which is consistent with the average crystallite size obtained from the peak broadening in XRD and Rietveld analysis. Fig. 5, inset shows the selected area electron diffraction pattern (SAED) of spinel $CdFe_2O_4$ NPs, which implies that the as-prepared samples are single crystalline in nature. SAED results show spotty ring characteristic of small crystallites of spinel ferrite nanostructure without any additional

diffraction spots and rings of secondary phases corresponding to the magnesium, nickel and iron oxides were observed.

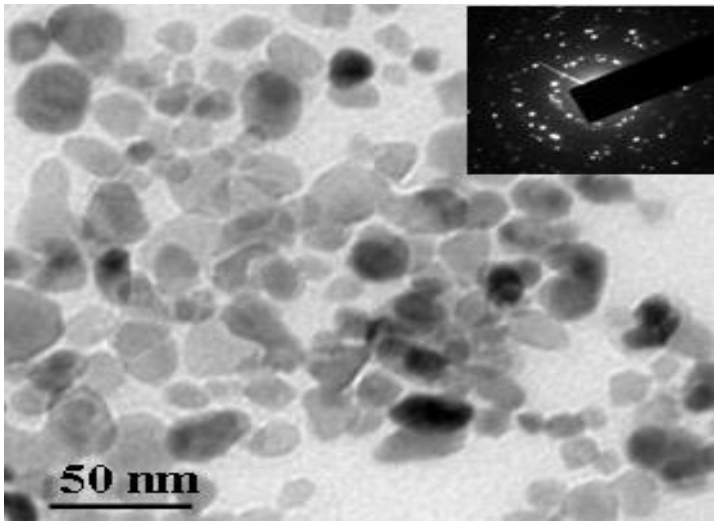

Fig. 5. HR-TEM images of $CdFe_2O_4$ powder.

3.6. VSM analysis

The magnetic (M-H) hysteresis curve obtained from VSM studies recorded at room temperature for $CdFe_2O_4$ powder synthesized via sol-gel method is shown in Fig. 6. It is observed that the magnetic properties show dependence on particle size, morphology, methods of preparation etc. Moreover, the sample shows the superparamagnetic nature. Also, indicated that the sample is soft magnetic character, because of very low remanent and coercivity values, which is close to the saturation magnetisation of bulk $CoFe_2O_4$ ferrite.

e-ISSN 2320 –7876 www.ijfans.org
Vol.11, Iss.9, Dec 2022

Research Paper

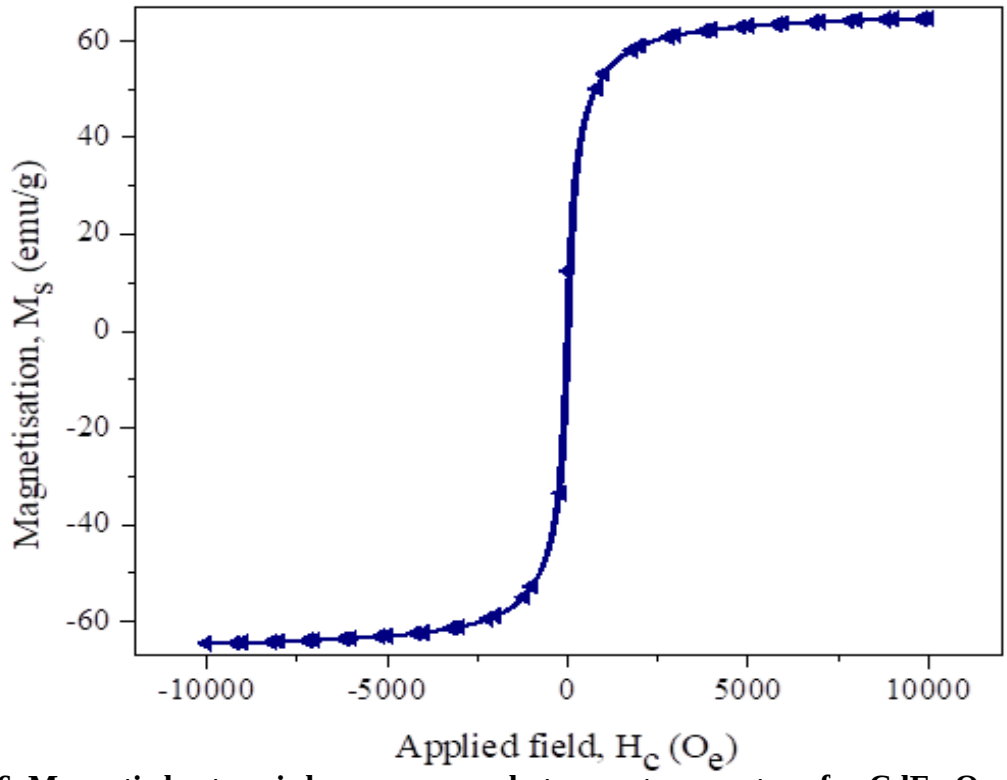

Fig.6. Magnetic hysteresis loops measured at room temperature for $CdFe_2O_4$ powder synthesized by sol–gel method

4. Conclusions

Spinel $CoFe_2O_4$ nanoparticles were synthesized by sol–gel method. HR-SEM images has been used to study their morphology and resulted in the formation of well dispersed $CoFe_2O_4$ particles with spherical shaped morphology. Magnetic hysteresis loop confirmed the suoerparamagnetic nature of the sample which was recorded using vibrating sample magnetometer. Moreover, this method gives wider scope to study about the synthesis methods for the preparation of spinel magnetic nanomaterials with low cost and easy process.

References

[1]. Y. S. Kim, H. J. Chae, S. J. Seo, K. T. Park, B. S. Kim, and T. S. Kim, Prediction of Diffusion Behaviors Between Liquid Magnesium and Neodymium-Iron-Boron Magnets, Sci. Adv. Mater. vol. 8, 134-137 (2016)

[2]. A. Baykal, I.A. Auwal, S. Güner, and H. Sözeri, Magnetic and optical properties of Zn^{2+} ion substituted barium hexaferrites, J. Magn. Magn. Mater. vol. 430, 29–35 (2017)

[3]. A. Baykal, Ş. Eryiğit, R. Topkaya, H. Güngüneş, Md. Amir, A. Yıldız, U. Kurtan, and Sagar E. Shirsath, Magnetic properties and hyperfine interactions of $Co_{1-2x}Ni_xMn_xFe_2O_4$ nanoparticles, Ceram. Int., vol. 43, 4746–4752 (2017)

[4]. H. Sözeri, F. Genç, B. Ünal, A. Baykal, and B. Aktaş, Magnetic, electrical and microwave properties of Mn–Co substituted $Ni_xZn_{0,8-x}Fe_2O_4$ nanoparticles, J. Alloys Compd., vol. 660, 324–335 (2016)

[5]. C. Sasikala, N. Durairaj, I. Baskaran, B. Sathyaseelan, M. Henini, and E. Manikandan, Transition metal titanium (Ti) doped $LaFeO_3$ nanoparticles for enhanced optical structural and magnetic properties, J. Alloys Compd. vol. 712, 870–877 (2017).

[6]. R. Sharma, P. Thakur, P. Sharma, and V. Sharma, Ferrimagnetic Ni^{2+} doped Mg-Zn spinel ferrite nanoparticles for high density information storage, J. Alloys Compd. vol. 704, 7–17 (2017)

[7]. U.R. Ghodake, Rahul.C. Kambale, and S.S. Suryavanshi, Effect of Mn^{2+} substitution on structural, electrical transport and dielectric properties of Mg-Zn ferrites, Ceram. Int., vol. 43, 1129–1134 (2017)

[8]. H. Bahiraeia, and C.K. Ong, Microstructural and electromagnetic study of low temperature fired nano crystalline MgCuZn ferrite with Bi_2O_3 addition, Ceram. Int. vol. 43, 4780–4784 (2017)

[9]. W. C. Hsu, S.C. Chen, P.C. Kuo, C.T. Lie, and W.S. Tsai, Preparation of NiCuZn ferrite nanoparticles from chemical co-precipitation method and the magnetic properties after sintering, Mater. Sci. Eng., vol. 111, 142-149 (2004)

[10]. H. Su, H. Zhang, X. Tang, B. Liu, and Z. Zhong, Effects of Co-substitution on DC-bias-superposition characteristic of the NiCuZn ferrites, Physica B, vol. 405, 4006-4009 (2010)

[11]. Y.M. Al Angari, Magnetic properties of La-substituted $NiFe_2O_4$ via egg-white precursor route, J. Magn. Magn. Mater. vol. 323, 1835-1839 (2011)

[12]. R. Desai, R. V. Mehta, R. V. Upadhyay, A. Gupta, A. Praneet, and K. V. Rao, Bulk magnetic properties of $CdFe_2O_4$ in nano-regime, Bulletin of Materials Science, 30 (2007) 197–203.

[13]. Y. Sharma, N. Sharma, G. V. S. Rao, and B. V. R. Chowdari, Li-storage and cycling properties of spinel, $CdFe_2O_4$, as an anode for lithium ion batteries, Bulletin of Materials Science, 32 (2009) 295–304.

[14]. E.R. Kumar, R. Jayaprakash, and S. Kumar, Effect of annealing temperature on structural and magnetic properties of manganese substituted $NiFe_2O_4$ nanoparticles, Mater. Sci. Semicond. Proces. vol. 17, 173-177 (2014)

[15]. R. Topkaya, H. Güngüneş, Ş. Eryiğit, Sagar E. Shirsath, A. Yıldız, and A. Baykal, Effect of bimetallic (Ni and Co) substitution on magnetic properties of $MnFe_2O_4$ nanoparticles, Ceram. Int. vol. 42, 13773-13782 (2016)

[16]. K. Panwar, S. Tiwari, K. Bapna, N.L. Heda, R.J. Choudhary, D.M. Phase, and B.L. Ahuja, The effect of Cr substitution on the structural, electronic and magnetic properties of pulsed laser deposited $NiFe_2O_4$ thin films, J. Magn. Magn. Mater. vol. 421, 25-30 (2017)

[17]. L. Chen, Y. Shen, and J. Bai, Large-scale synthesis of uniform spinel ferrite nanoparticles from hydrothermal decomposition of trinuclear heterometallic oxo-centered acetate clusters, Mater. Lett. vol. 63, 1099–1101 (2009)

[18]. W. X. Hou, and Z. Wang, Mater. Structural and magnetic properties of $Ni_{0.15}Mg_{0.1}Cu_{0.3}Zn_{0.45}Fe_2O_4$ ferrite prepared by NaOH-precipitation, Sci. Eng. B vol. 199, 57–61 (2015)

[19]. B. H. Anilkumar and K. S. Venkatesh, Dielectric Study of Polyaniline/$NiFe_2O_4$ Composites Prepared by Reflux Techniques, Mater. Focus vol. 5, 476–480 (2016)

[20]. A. Ghasemi, A. Ashrafizadeh, A. Paesano Jr., C. F. Cerqueira Machado, S. E.Shirsath, X. Liu, and A. Morisako, The role of copper ions on the structural and magnetic characteristics of MgZn ferrite nanoparticles and thin films, J. Magn. Magn. Mater. vol. 322, 3064–3071 (2010)

[21]. X. Liang, J. Huang, W. Li, and H. Zeng, Enhancing Coloring Performance of Submicron $ZnFeCrO_4$ Brown Pigment with Modified Gel-Casting Method, Sci. Adv. Mater. vol. 8, 1563–1570 (2016)

[22]. C.C. Hwang, J. Tsai, and T.H. Huang, Combustion synthesis of Ni-Zn ferrite by using glycine and metal nitrates-investigation of precursor homogeneity, product reproducibility, and reaction mechanism, J. Mater Chem. Phy., vol. 93, 330–336 (2005)

[23]. R. P. Patil, R. S. Pandav, A. V. Jadhav, S. D. Jadhav, and P. P. Hankare, Investigation of Structural, Magnetic and Photocatalytic Properties of Al Substituted Cobalt Ferrites, Mater. Focus vol. 5, 11-16 (2016)

[24]. L. Wu, C. Dong, C. Zhang, C. Jiang, and D. Xue, Voltage-Controlled Bistable Resistive Switching Behavior Based on $Ni_{0.5}Zn_{0.5}Fe_2O_4/BiFeO_3/Nb:SrTiO_3$ Heterostructures, Sci. Adv. Mater. vol. 8, 712-717 (2016)

[25]. A. Verma, O.P. Thakur, C. Prakash, T.C. Goel, and R.G. Mendiratta, Temperature dependence of electrical properties of nickel–zinc ferrites processed by the citrate precursor technique, Mater. Sci. Eng. B, vol. 116, 1–6 (2005).

[26]. S. Rehman, M. A. Almessiere, S. S. Al-Jameel, U. Ali, Y. Slimani, N. Taskhandi, N. S. Al-Saleh, A. Manikandan, F. A. Khan, E. A. Al-Suhaimi, A. Baykal, Designing of $Co_{0.5}Ni_{0.5}Ga_xFe_{2-x}O_4$ ($0.0 \leq x \leq 1.0$) Microspheres via Hydrothermal Approach and Their Selective Inhibition on the Growth of Cancerous and Fungal Cells, Pharmaceutics, 13 (2021) 962.

[27]. M. A. Almessiere, B. Unal, Y. Slimani, H. Gungunes, M. S. Toprak, N. Tashkand, A. Baykal, M. Sertkol, A.V. Trukhanov, A. Yıldız, A. Manikandan, Effects of Ce-Dy rare earths co-doping on various features of Ni-Co spinel ferrite microspheres prepared via hydrothermal approach, J. of Materials Research and Technology, 14 (2021) 2534-2553.

[28]. S. Blessi, A. Manikandan, S. Anand, M. M. L. Sonia, V. M. Vinosel, P. Paulraj, Y. Slimani, M.A. Almessiere, M. Iqbal, S. Guner, A. Baykal, Effect of Zinc substitution on the physical and electrochemical properties of mesoporous SnO_2 nanomaterials, Materials Chemistry and Physics, 273 (2021) 125122.

[29]. M. A. Almessiere, Y. Slimani, Y. O. Ibrahim, M. A. Gondal, M. A. Dastageer, I. A. Auwal, A. V. Trukhanov, A. Manikandan, A. Baykal, Morphological, structural, and magnetic characterizations of hard-soft ferrite nanocomposites synthesized via pulsed laser ablation in liquid, Materials Science and Engineering B, 273 (2021) 115446.

[30]. S. Blessi, S. Anand, A. Manikandan, M. Maria Lumina Sonia, V. Maria Vinosel, Y. Slimani, M.A. Almessiere, A. Baykal, Influence of Ni substitution on opto-magnetic and electrochemical properties of CTAB capped mesoporous SnO_2 nanoparticles, Journal of Materials Science: Materials in Electronics, Journal of Materials Science: Materials in Electronics, 32 (2021) 7630–7646.

[31]. M. George, T.L. Ajeesha, A. Manikandan, Ashwini Anantharaman, R.S. Jansi, E. Ranjith Kumar, Y. Slimani, M.A. Almessiere, A. Baykal, Evaluation of Cu-$MgFe_2O_4$ spinel nanoparticles for photocatalytic and antimicrobial activates, Journal of Physics and Chemistry of Solids, 153 (2021) 110010.

[32]. S. Güner, A. Baykal, Md. Amir, H. Güngüneş, M. Geleri, H. Sözeri, Sagar E. Shirsath, and M. Sertkol, Synthesis and characterization of oleylamine capped $Mn_xFe_{1-x}Fe_2O_4$ nanocomposite: Magneto-optical properties, cation distribution and hyperfine interactions, J. Alloys Compd., vol. 688, 675–686 (2016)

[33]. M. AsifIqbal, M.U. Islam, Irshad Ali, Muhammad Azhar Khan, Shahid M. Ramay, and M. Hassan, Study of physical, magnetic and electrical properties of rare-earth substituted Li-Mg ferrites, J. Alloys Compd., vol. 692, 322–331 (2017)

[34]. U.R. Ghodake, N.D. Chaudhari, R.C. Kambale, J.Y. Patil, and S.S. Suryavanshi, Effect of Mn^{2+} substitution on structural, magnetic, electric and dielectric properties of Mg–Zn ferrites, J. Magn. Magn. Mater. vol. 407, 60–68 (2016)